Ecotoxicology and Environmental Safety 169 (2019) 960–970

Contents lists available at ScienceDirect

Ecotoxicology and Environmental Safety

journal homepage: www.elsevier.com/locate/ecoenv

Immediate and legacy effects of urban pollution on river ecosystem functioning: A mesocosm experiment

Olatz Pereda[a,*], Vicenç Acuña[b], Daniel von Schiller[a], Sergi Sabater[b,c], Arturo Elosegi[a]

[a] Faculty of Science and Technology, the University of the Basque Country (UPV/EHU), PO Box 644, 48080 Bilbao, Spain
[b] Catalan Institute for Water Research (ICRA), Carrer Emili Grahit 101, 17003 Girona, Spain
[c] Institute of Aquatic Ecology, University of Girona, Campus de Montilivi, 17071 Girona, Spain

ARTICLE INFO

Keywords:
WWTP effluent
Pollution gradient
Subsidy-stress
Artificial stream
Biofilm
Ecosystem functioning

ABSTRACT

Effluents from urban wastewater treatment plants (WWTP) consist of complex mixtures of substances that can affect processes in the receiving ecosystems. Some of these substances (toxic contaminants) stress biological activity at all concentrations, while others (*e.g.*, nutrients) subsidize it at low concentrations and stress it above a threshold, causing subsidy-stress responses. Thus, the overall effects of WWTP effluents depend mostly on their composition and the dilution capacity of the receiving water bodies. We assessed the immediate and legacy effects of WWTP effluents in artificial streams, where we measured the uptake of soluble reactive phosphorus (SRP) by the biofilm, biomass accrual, benthic metabolism and organic matter decomposition (OMD). In a first phase (32 d), the channels were subjected to a gradient of effluent contribution, from pure stream water to pure effluent. WWTP effluent affected the ecosystem processes we measured, although we found no clear subsidy-stress patterns except for biofilm biomass accrual. Instead, most of the processes were subsidized, although they showed complex and process-specific patterns. Benthic metabolism and OMD were subsidized without saturation, as they peaked at medium and high levels of pollution, respectively, but they never fell below control levels. SRP uptake was the only process that decreased with increasing effluent concentration. In a second phase of the experiment (23 d), all channels were kept on pure stream water to analyse the legacy effects of the effluent. For most of the processes, there were clear legacy effects, which followed either subsidy, stress, or subsidy-stress patterns. SRP uptake capacity was stressed with increasing pollution legacy, whereas algal accrual and benthic metabolism continued being subsidized. Conversely, biofilm biomass accrual and OMD showed no legacy effects. Overall, the WWTP effluent caused complex and process-specific responses in our experiment, mainly driven by the mixed contribution of subsidizers and stressors. These results help improving our understanding of the effects of urban pollution on stream ecosystem functioning.

1. Introduction

Cities have been expanding exponentially as a consequence of population growth and migration from rural to urban areas (Jones and O´Neill, 2016). Associated to urban growth, inputs of sewage water, either raw or treated in waste water treatment plants (WWTPs), are a relevant point-source pollution in river ecosystems (Vörösmarty et al., 2010). WWTPs reduce urban pollution (Tchobanoglous and Burton, 1991; Serrano, 2007), but their effluents still contribute complex mixtures of substances including organic matter, nutrients (Carey and Migliaccio, 2009; Martí et al., 2009), metals, pesticides and emergent pollutants such as pharmaceuticals, personal care products, or even illicit drugs (Gros et al., 2007; Santos et al., 2013; Rosi-Marshall et al., 2015; Aymerich et al., 2017). Given their content of assimilable and toxic compounds, they could either subsidize ecosystem processes or stress them (*sensu* Odum et al., 1979) depending on their exact composition and final concentration (Cardinale et al., 2012; Rice and Westerhoff, 2017), as well as on the composition of the biological communities receiving the effluents (Segner et al., 2014). Therefore, the ecological effects of these effluents are still far from clear (Aristi et al., 2015). For instance, inorganic nutrients promote (subsidize) biological activity up to a threshold where they become toxic and start reducing it below "normal" levels (stress), whereas most heavy metals, pesticides or even antibiotics tend to suppress biological activity roughly in proportion to their concentration (Rodríguez-Mozaz and Weinberg, 2010; Peters et al., 2013). Both assimilable and toxic compounds impair water quality (Beyene et al., 2009; Ribot et al., 2012), alter the structure of biological communities (Bundschuh et al., 2011; Drury et al., 2013;

* Corresponding author.
E-mail address: olatz.pereda@ehu.eus (O. Pereda).

https://doi.org/10.1016/j.ecoenv.2018.11.103
Received 8 October 2018; Received in revised form 20 November 2018; Accepted 22 November 2018
Available online 12 December 2018

Rosi-Marshall et al., 2015), and affect the rates of different ecosystem processes (Aristi et al., 2015; Corcoll et al., 2015). On the other hand, the final concentration of these effluents depends on the dilution capacity of the receiving water body, which can be affected by human activities such as water abstraction (Arroita et al., 2016), or climate change (Hisdal et al., 2001; Englert et al., 2013).

Ecosystem functioning reflects the fluxes of energy and matter in ecosystems (Tilman et al., 2014; von Schiller et al., 2017). Although explicitly included in the EU Water Framework Directive (WFD), which defines ecological status as "an expression of the structure and functioning of aquatic ecosystems associated with surface waters", ecosystem functioning is seldom considered in current monitoring schemes (Birk et al., 2012). In addition to being an essential component of ecosystem health, it is at the basis of the services provided by river ecosystems (Millennium Ecosystem Assessment, 2005). However, we still largely ignore how ecosystem functioning responds to WWTP effluents and their potential legacy effects. Contradictory responses have been reported depending on the processes measured; for instance, organic matter decomposition (OMD) increases in stream reaches receiving effluent inputs (*e.g.* Pascoal et al., 2003), whereas nutrient retention is either unaffected (Haggard et al., 2001, 2005) or even reduced after receiving WWTP effluents (Martí et al., 2004; Merseburger et al., 2005, 2011). Besides, responses on autotrophic and heterotrophic processes may differ when effects are estimated at the site or are upscaled to the whole-ecosystem (*e.g.* Aristi et al., 2015). Also the experimental duration may influence the pattern of response (Aristi et al., 2016). Finally, effects may persist even when effluents are no longer received, producing a legacy which delays the recovery capacity of the ecosystem. Although the legacy effects of stressors are widely recognised (Holeton et al., 2011; Sharpley et al., 2013), very few works have experimentally addressed this issue (Alvarez et al., 2014).

The effects of WWTP effluents on ecosystem functioning depend on their final concentration in the receiving water, and thus, are difficult to assess in the real world. This situation prompts for laboratory experiments under controlled conditions, allowing for a mechanistic understanding that otherwise would remain elusive in field conditions (Benton et al., 2007). In the case of river ecosystems, artificial indoor channels have been used to unveil complex ecological phenomena. For instance, the interaction between nutrients and emerging contaminants (Aristi et al., 2016), the importance of the duration of non-flow periods in intermittent waterways (Acuña et al., 2015), the effect of altered diel temperature patterns associated to global warming (Freixa et al., 2017), or the effects of pharmaceuticals and illicit drugs on stream biological communities (Hoppe et al., 2012; Lee et al., 2016).

We investigated the impact of WWTP effluents on ecosystem processes by conducting a laboratory experiment using artificial streams, in which potentially confounding environmental factors were strongly simplified. We aimed at testing the following predictions: (1) biological processes would respond to the gradient of effluent dilution capacity following a subsidy-stress scheme, *i.e.*, showing an increase at low to moderate proportions of effluent, but a decrease below control (pure stream water) levels at high proportions; (2) the response pattern would diverge among processes; and (3) the effluent would produce legacy effects, *i.e.*, affect the recovery capacity of the process, in a way roughly proportional to the effluent concentration.

2. Material and methods

2.1. Experimental design

We conducted an experiment using a series of artificial streams located in the indoor Experimental Streams Facility of the Catalan Institute for Water Research (Girona, Spain). Each artificial stream was assigned to one of eight treatments, from non-polluted water (control treatment) to pure WWTP effluent (0%, 14%, 29%, 43%, 58%, 72%, 86% and 100% of WWTP effluent water). We used three replicates per treatment (8 treatments × 3 replicates = 24 artificial streams) distributed in four separate arrays of six artificial streams, with each treatment represented only once per array. The dilution values were designed to represent a regression design (Navarro et al., 2000) from an unpolluted stream scenario with no WWTP contribution, to a temporary stream scenario during the dry phase, when 100% of the water flow comes from the WWTP effluent. The design was also aimed at detecting tip-points and thresholds between subsidy and stress for each of the measured processes.

The experiment was developed between January 19th and March 31st, 2017. After an acclimation phase of 15 d, artificial streams were subjected to the different treatments during a first exposure phase (32 d), followed by a recovery phase (23 d), in which the flow of clean water was restored in all the artificial streams. Other research performed in the same artificial channels (*e.g.*, Aristi et al., 2016; Freixa et al., 2017; Subirats et al., 2018) used previously sterilized sediment, which was left for 3 weeks to allow biofilm colonization. However, we used field-colonised sediment (see below) and thus, the colonized biofilms were left for 2 weeks for acclimation to the laboratory conditions. The duration of the exposure phase was fixed based on previous research in the channels, which showed a fast biofilm response under our experimental conditions. The recovery phase lasted for 23 days, which allowed us to measure short-term responses.

2.2. Experimental conditions

Each artificial stream consisted of an independent methacrylate channel (length-width-depth: 200 cm – 10 cm – 10 cm), and a 70-L water tank from which water was re-circulated. Each stream received a constant flow of 50 mL s^{-1} and operated as a closed system for 72 h, so all the water in each channel was renewed every three days. Water mean velocity was 0.71 cm s^{-1} and water depth over the plane bed ranged from 3 to 3.5 cm. Each artificial stream was filled with 5 L of sand and 14 cobbles collected from an unpolluted segment of the nearby Llémena River. The Llémena is a permanent Mediterranean oligotrophic calcareous stream, which has been previously used as a reference site for ecotoxicological laboratory experiments on biofilms due to its relatively low concentration of contaminants (Bonnineau et al., 2010; Serra et al., 2010; Corcoll et al., 2015). The sediment and cobbles were transported in less than 1 h to the artificial streams and evenly distributed to create a plane bed to facilitate biofilm growth. During the acclimation phase, the biofilm was allowed to grow on the artificial streams from the inoculum present in these sediments and cobbles. After the exposure phase, additional cobbles from the Llémena River were included in the channels to mimic colonization from upstream reaches.

The artificial streams were fed with rainwater filtered through activated carbon filters, and WWTP effluent water added to every set of them following the above dilution scheme. Treated effluents were collected at the WWTP of Quart (Girona, Spain), transported in 200-L tanks, and transferred to the artificial streams in less than 2 h. Daily cycles of photosynthetic active radiation (PAR) in the channels were defined as 10 h daylight (09:00–19:00) + 14 h darkness (19:00–09:00) using LED lights (120 W; Lightech, Girona, Spain). PAR was held constant at 174 ± 33 μE m^{-2} s^{-1} during the daytime and recorded every 10 min using 4 quantum sensors located across the whole array of streams (sensor LI-192SA, LiCOR Inc, Lincoln, USA). Air temperature was maintained at 10 °C during the acclimation phase and at 15 °C during the exposure and recovery phases, with an air humidity of 30%, to allow a gradual acclimation of the biofilm from the stream conditions to the artificial channel conditions. Additionally, water temperature was held constant at 20 °C over the whole experiment and it was recorded every 10 min using VEMCO Minilog temperature data loggers (−5 to 35 ± 0.2 °C) (TR model, AMIRIX Systems Inc, Halifax, NS, Canada). Overall, physico-chemical conditions in the artificial streams (water velocity, temperature and light cycles) emulated those of the

Llémena River during early spring.

2.3. Water chemistry

Background physico-chemical conditions [pH, temperature (T), conductivity and dissolved oxygen (DO) concentration and saturation] were measured at noon every 3–4 d from water collected on the channel outlet of each artificial stream using hand-held probes (WTW multiline 3310, Weilheim, Germany; YSI ProODO handled, YSI Inc., Yellow Springs, OH, USA). 24 h after the renewal of the artificial streams concentrations of nutrients, major anions and cations, and dissolved organic carbon (DOC) were measured from water collected from the channel outlet. Water for nutrient analyses was immediately filtered through 0.2-μm pore size nylon filters (Whatman, Kent, UK) into pre-washed polyethylene containers. The concentration of soluble reactive phosphorus (SRP) was determined colorimetrically using a fully automated discrete analyzer Alliance Instruments Smartchem 140 (AMS, Frépillon, France). The concentration of anions [nitrate ($N\text{-}NO_3^-$), nitrite ($N\text{-}NO_2^-$), sulphate (SO_4^{2-}), chloride (Cl^-) and bromide (Br^-)] and cations [ammonium ($N\text{-}NH_4^+$), calcium (Ca^{2+}), magnesium (Mg^{2+}), sodium (Na^+) and potassium (K^+)] were determined on a Dionex ICS-5000 ion chromatograph (Dionex Corporation, Sunnyvale, USA). Water for DOC analysis was immediately filtered through ashed 0.7-μm pore size glass fibre filters (Whatman GF/F, Kent, UK). The concentration of DOC was determined using a Shimadzu TOC-V CSH (Shimadzu Corporation, Kyoto, Japan). Heavy metal concentrations were analyzed on water samples of the most polluted treatment (100%) filtered through 0.45-μm pore size nylon filters (Whatman, Kent, UK) collected the last day of the first experimental phase (32 d) and determined by ICP-MS (7500c Agilent Technologies, Inc. Willington, DE).

2.4. Response processes

The stream ecosystem functional response was assessed by measuring the SRP uptake capacity (U_{SRP}) of the biofilm, its biomass accrual [Chlorophyll-*a* (Chl-*a*) and ash-free dry mass (AFDM)] and the metabolism of the benthic community [gross primary production (GPP) and community respiration (CR)]. The activity of the microbial heterotrophic community was also assessed by the capacity to consume available organic matter (organic matter decomposition, OMD).

2.4.1. Biofilm SRP uptake and biomass accrual

SRP uptake and biomass accrual of the biofilm were measured on artificial substrata known as biofilm carriers, which have been used elsewhere (Baldwin et al., 2003; Elosegi et al., 2018). These are artificial plastic substrata with a high surface-to-volume ratio, which are used in WWTPs and aquaria to encourage biofilm attachment. We used cubic polyethylene carriers 2.5 cm in side (SERA GmbH D52518, Heinsberg, Germany), deployed at the beginning of the exposure phase and wired to each of the streams in batches of 8 cubes. At the end of each phase (32 d and 55 d of incubation), we recovered 1 biofilm carrier per stream (3 replicates per treatment), which were immediately subjected to a bioassay to measure SRP uptake capacity (see below, in the same section) and then frozen in individual labelled plastic bags. After thawing, biofilm was detached from the biofilm carrier using a Branson sonifier ultrasonic cell disruptor (Branson Ultrasonic TM, Branson Ultrasonic Corporation, Emerson Electric, USA) combining 3 min of pulse mode at 70% of amplitude and 2 min of continuous mode at the same amplitude in 100 mL of deionized water. The biofilm solution was filtered onto ashed 0.7-μm pore size glass-fibre filters (Whatman GF/F, Kent, UK) for the determination of Chl-*a* and AFDM.

The SRP uptake capacity (U_{SRP}) of the biofilm growing on the biofilm carriers was measured by a method adapted from Elosegi et al. (2018). Briefly, once the biofilm carriers were collected from each channel, they were individually incubated in 100-mL clean plastic vials with an acclimation solution (1:5 dilution of Perrier carbonated mineral water (Nestlé, France) in deionized water), designed to ensure a sufficient supply of micronutrients, for 30 min at 100 rpm shaking speed, 20 °C and ~ 180 μmol m^{-2} s^{-1} light. After the acclimation phase, the biofilm carriers were placed individually in pre-washed 60-mL plastic vials with the same acclimation solution but spiked with a PO_4 solution (K_2HPO_4, 10 mM = 310 mg P L^{-1}) to achieve a final concentration of 5 μM P (155 μg P L^{-1}), and incubated under the same conditions for 1 h. This concentration was chosen as a compromise to ensure saturating conditions for the biofilm while allowing the nutrient decline during the incubation and the subsequent estimation of uptake. After the incubation, 20 mL of water were collected from each vial, and 10 mL were filtered through glass-fibre filters (0.7-μm pore size, Whatman GF/F, Kent, UK) into 15-mL plastic tubes and frozen until analysis. Together with the colonized substrates, control treatments using non-colonized biofilm carriers (n = 3 on each incubation) were also used. The SRP uptake capacity was calculated as the difference between the mean SRP concentration of the control treatments (non-colonized substrates) and the colonized substrates, in the incubation solution volume (L) per incubation time (h). Thus, uptake capacity results were expressed in μg P h^{-1}. SRP uptake capacity was also standardized by the biofilm biomass (AFDM) to obtain a clear picture about the efficiency of the biofilm to take up phosphorus. SRP concentration was determined manually on a double-beam UV-1800 UV–Vis Spectrophotometer (Shimadzu, Shimadzu Corporation, Kyoto, Japan) following the method described by Murphy and Riley (1962). The high N/P ratio in our channels suggested phosphorus to be the limiting nutrient.

Chl-*a* was measured for each filter after extraction in 90% acetone for 12 h in the dark at 4 °C (Steinman et al., 2006). To ensure the complete extraction of Chl-*a*, samples were sonicated for 30 s, twice (30 s, 360 W power, 50/60 Hz frequency, JP Selecta S.A., Barcelona, Spain). After that, Chl-*a* concentration was determined spectrophotometrically (U-2000 Spectrophotometer; Hitachi, Tokyo, Japan) by measuring the absorbance at 665 and 750 nm wavelengths, following the method described in Jeffrey and Humphrey (1975). Results were expressed as μg of Chl-*a* cm^{-2} of biofilm carrier surface area. Besides, AFDM was used as an estimate of biofilm biomass. For its determination, another subsample of the biofilm extract was filtered on pre-weighed filters, dried at 70 °C for 72 h to constant weight, weighed, combusted at 500 °C for 5 h using a muffle furnace (AAF 1100, Carbolite, UK) and reweighed. Results were expressed as mg of AFDM cm^{-2} of biofilm carrier surface area.

2.4.2. Benthic metabolism

We measured biofilm net community metabolism (NCM) and community respiration (CR) by analysing the changes in DO concentration inside cylindrical (0.96 L) recirculating chambers, as described by Acuña et al. (2008). One tray (64 cm^2 in surface area) made of stainless-steel wire mesh (1 mm mesh size) was located on each channel at the beginning of the acclimation phase to allow for a gradual biofilm adaptation. All the trays were filled with coarse sand (d_{50} = 0.74 mm median diameter grain size (48 cm^2 surface area)) and included a pebble *c.a.* 4.5-cm in diameter (16 cm^2 surface area), to collect the performance of epipsammic and epilythic biofilm. At the end of each phase, trays were extracted from the channels, placed in the recirculating chambers, filled with water from the corresponding treatment and incubated for 1 h in light plus 1 h in darkness. All the chambers were deployed inside an incubator chamber (Radiber AGP-700-ESP, Barcelona, Spain) to maintain the water temperature equal to that in the artificial streams (20 °C). NCM was measured under light conditions (constant PAR of 168 ± 2 μE m^{-2} s^{-1}, similar to the irradiance at the artificial streams), while CR was measured in darkness. Once metabolism measurements were performed, trays were returned to their corresponding artificial stream. DO concentration inside the chambers was measured every 15 s with oxygen sensors (PreSens OXY-10mini, Regensburg, Germany). Metabolism rates were calculated following Acuña et al. (2008), in which NCM and CR were computed from

the difference in oxygen concentration between two consecutive measurements (mg O_2 L^{-1}), in a specific time interval (h), accounting for the water volume used in the chamber (L) and the active surface of the substrate used for the incubation (m^2). Gross primary production (GPP) was estimated as the sum of NCM and CR. In all cases, results were expressed in mg O_2.

2.4.3. Organic matter decomposition

We measured OMD using 12-mm diameter discs from freshly fallen leaves of black alder (*Alnus glutinosa* (L.) Gaertner). Discs were cut using a cork borer, arranged in sets of 15, and each set was weighed and enclosed in black PVC tubes to prevent algal growth. PVC tubes (2 cm diameter and 5 cm long) were individually labelled and covered with a fine mesh (400 μm mesh size) to preclude losing the discs while allowing microbial colonization and water flow. PVC tubes were placed flat and longitudinally on the bed of the artificial streams at the beginning of the exposure phase in groups of 9, which allowed having 3 replicates per channel. At the end of the exposure phase, leaf discs inside PVC tubes were collected, oven-dried (72 h, 70 °C), weighed, combusted (5 h, 500 °C) and weighed again to estimate AFDM. In the recovery phase, the same process was repeated with another set of discs previously prepared under the same conditions. To correct the initial mass of the leaves used during the experiment, the leaching rate was determined in the laboratory from an additional set of 20 tubes (10 per each experimental phase) incubated under the same experimental conditions. Decomposition rates were calculated according to the negative exponential model (Petersen and Cummins, 1974), and were expressed as d^{-1}.

2.5. Data analysis

We aimed at identifying the response type of the functional processes we measured by comparing the fit of 8 different models (linear, exponential, power, logistic, logit, Monod, Haldane and quadratic, Table 1, Fig. S1) to the data. These models were selected to encompass the most common relationships between ecosystem processes and environmental factors. The linear and quadratic models were adjusted using linear models with the "lm" R function (Chambers, 1992), whereas the other models were adjusted using non-linear models with generalized least squares by the "gnls" R function (Pinheiro et al., 2018). The number of models fitted was not the same for all the variables, as the specific conditions necessary to run some of the models were not always fulfilled. Thus, results for the models [*i.e.*, Akaike Information Criterion (AIC) and Relative Standard Errors (RSE)] were only computed when the data of each variable fulfilled these conditions. However, the simplest response (the linear model) was always computed. Among all the computed models, we selected the most appropriate in each case following a standard selection criterion: 1) lowest AIC value, 2) lowest RSE value and 3) the model computed must have ecological sense. This means that models without ecological sense, such as inverse Haldane or Quadratic models, although computed, were disregarded. Equally, when none of the models fit the data, the linear model was selected by default. Normality of the residuals was checked for the adjusted models in each case, to ensure a correct utilization of the AIC values. Pearson moment correlation analyses were also used with the averaged values of water characteristics (*i.e.*, physico-chemical variables and concentrations of nutrients, anions and cations and DOC) to identify the direction and strength of the response to the gradient of WWTP effluent. All statistical analyses were performed using R software, ver. 3.4.0. (R Core Team, 2017).

3. Results

3.1. Water chemistry

The effluent used throughout the experiment had 7.9 ± 0.1 pH, 1348 ± 61 μS cm^{-1} conductivity and 6.9 ± 0.4 mg L^{-1} DO. Nutrient and DOC concentrations were high: 5.8 ± 2.0 mg N L^{-1} of $N\text{-}NO_2^-$, 16.1 ± 3.2 mg N L^{-1} of $N\text{-}NH_4^+$, 16.1 ± 4.2 mg N L^{-1} of $N\text{-}NO_3^-$, 0.70 ± 0.13 mg P L^{-1} of SRP and 14.3 ± 0.5 mg C L^{-1} of DOC (see Table 2 and Table S1 for more details). Copper (81.9 ± 1.6 μg L^{-1}), zinc (71.8 ± 4.8 μg L^{-1}), iron (51.9 ± 3.9 μg L^{-1}) and arsenic (7.3 ± 0.2 μg L^{-1}) were the most abundant heavy metals in the effluent (Table S1). Increased effluent contribution linearly reduced DO and pH (R^2 = 0.87, $p < 0.001$ and R^2 = 0.93, $p < 0.001$, respectively), and increased conductivity (R^2 = 0.99, $p < 0.001$), nutrients (R^2 = 0.94, $p < 0.001$ for $N\text{-}NO_2^-$; R^2 = 0.99, $p < 0.001$ for $N\text{-}NH_4^+$; R^2 = 0.98, $p < 0.001$ for $N\text{-}NO_3^-$; R^2 = 0.95, $p < 0.001$ for SRP) and DOC concentration (R^2 = 0.99, $p < 0.001$). However, T did not vary between treatments (R^2 = 0.01, p = 0.84; Table 3). The solutes increased linearly but in different proportion: $N\text{-}NO_2^-$ increased up to 100-fold, $N\text{-}NH_4^+$ up to 400-fold, whereas $N\text{-}NO_3^-$, SRP and DOC increased up to 5- to 20-fold. The entrance of unpolluted water in the recovery phase eliminated the differences among treatments (Table 2).

3.2. Biofilm SRP uptake and biomass accrual

The WWTP effluent caused an immediate stress effect on SRP uptake capacity, which peaked in the control treatment (5.6 μg P h^{-1}, 0%) and decreased with increasing pollution proportions (Fig. 1a) to the point that above 70% of effluent contribution, it became negative, *i.e.* biofilm carriers released SRP (Fig. 1a, b). This decrease in the uptake capacity followed a logit model (Table 3, Fig. S2), showing an abrupt decrease at the lower levels of pollution and a more stable but negative response from medium levels of effluent contribution. The effluent also caused important legacy effects on SRP uptake capacity, which followed the same decreasing pattern from the control treatment (5.7 μg P h^{-1}, 0%) to the most polluted one (1.4 μg P h^{-1}, 100%), fitting again the logit model (Table 3, Fig. S2).

The immediate effects of the WWTP effluent on biofilm SRP uptake efficiency (*i.e.*, uptake capacity standardized by biofilm biomass) consisted on a decrease (Fig. 1b), which was again highest in the control treatment (1.0 μg P mg $AFDM^{-1}$ h^{-1}, 0%), and decreased down to −0.2 μg P mg $AFDM^{-1}$ h^{-1} in the most polluted treatment. Once more, data fitted best the logit model (Table 3, Fig. S3), suggesting a pure stress effect. Legacy effects also peaked at low levels of effluent contribution (highest uptake: 0.8 μg P mg $AFDM^{-1}$ h^{-1}, 14%; lowest uptake: 0.2 μg P mg $AFDM^{-1}$ h^{-1}, 100%). This relationship, however, followed the Haldane model, which suggested a possible subsidy-stress legacy effect (Table 3, Fig. S3).

Maximum Chl-*a* values during the exposure phase occurred at medium levels of effluent contribution (17.5 μg cm^{-2}, 29%, Fig. 1c), while the lowest values (3.9 μg cm^{-2}) were observed in the control treatment. Thus, the immediate effects of pollution consisted on subsidizing Chl-*a* at all proportions of pollution tested. The data fitted best the Haldane model (Table 3, Fig. S4), thus suggesting a saturating subsidy effect which became inhibited at higher levels of effluent contribution. The WWTP effluent had a noticeable legacy effect on Chl-*a*, as values were lower in the control treatment (14.9 μg cm^{-2}) and peaked at intermediate levels of pollution (45.1 μg cm^{-2}, 58%). However, although the pattern was best described by the quadratic model (Table 3, Fig. S4), the falling limb of the hump did not fall below the control. This showed again a saturating subsidy legacy effect with inhibition due to the legacy of higher levels of pollution.

Immediate effects of pollution on biofilm biomass accrual (AFDM) suggested a subsidy-stress response (Fig. 1d): AFDM peaked at low-medium levels of effluent (1.8 mg cm^{-2}, 14%) and the lowest values occurred in the most polluted treatment (0.9 mg cm^{-2}), the data fitting best the Haldane model (Table 3, Fig. S5). Thus, AFDM showed a saturating subsidy effect which became stressed in the highest levels of effluent contribution. Pollution also showed important legacy effects for AFDM, as biofilm biomass accrual peaked in treatments previously

Table 1
Conception of the different models tested, with their corresponding mathematical equations, the meaning of the parameters on each equation, their ecological interpretation in our experiment and some examples from the literature describing each type of response. The y variable corresponds to the measured functional process, while the x variable represents effluent concentration.

Model	Equation	Parameters	Interpretation	References
Linear	$y = a + bx$	**a**, intercept - rate at concentration 0 **b**, slope	Functional response changes at a constant rate with effluent concentration, showing either direct subsidy (positive slope) or stress (negative slope).	Wagenhoff et al. (2011); Aristi et al. (2016)
Exponential	$y = ae^{bx}$	**a**, rate at concentration 0 **b**, increase rate	Subsidy or stress effects increase by equal ratio with each increase in effluent concentration	Vandermeer (2010); Wagenhoff et al., (2011, 2012)
Power	$y = ax^b$	**a**, coefficient **b**, exponent (defines curvature of function)	Subsidy or stress effects increase potentially with effluent concentration	Peters (1983); Marquet et al. (2005)
Logistic	$y = \frac{a}{1+e^{-b(x-x_0)}}$	**a**, maximum rate **b**, slope of the curve $\mathbf{x_0}$, **x** value of the sigmoid's midpoint	Subsidy effect initially increases exponentially but then levels because of a limiting factor	Ricklefs (1967); Vandermeer (2010); Wagenhoff et al. (2011)
Logit	$y = y_0 + \frac{1}{b} + \log\frac{x+1}{a-(x+1)}$	**a**, maximum rate **b**, slope of the curve $\mathbf{y_0}$, **y** value of the inverse sigmoid´s midpoint	Inverse to the logistic, it shows stress to increase exponentially with concentration until it levels	McFadden (1974); Hanley et al. (1998); Carl and Kühn (2007)
Monod	$y = a\frac{x}{b+x}$	**a**, maximum rate **b**, concentration value when the rate is at its half maximum	Similar to Michaelis-Menten equation, describes a subsidy effect that saturates as effluent concentration increases	Monod (1949); Mogens et al. (2000)
Haldane	$y = a\frac{x}{b+x+\frac{x^2}{c}}$	**a**, maximum rate **b**, concentration value when the rate is at its half maximum **c**, concentration value when the inhibition is at its half maximum	Subsidy-stress dynamics: functional response peaks at intermediate effluent concentrations but falls below normal at high concentrations. Rising and falling limbs can be asymmetric	Haldane (1930); Camargo and Alonso (2006); Woodward et al. (2012); Wagenhoff et al., (2011, 2012, 2013)
Quadratic	$y = ax^2 + bx + c$	**a**, concentration values when the inhibition is maximum **b**, slope **c**, intercept, the rate at concentration zero	Similar to Haldane, but the rising and falling limbs are symmetric	Otto and Day (2007); Weir and Pettit (2000); Austin (2002)

Table 2
Water characteristics in each treatment during the exposure and the recovery phases (all treatments pooled). Values shown are mean ± standard error (SE) calculated for pH, T, conductivity and DO concentration from 3 replicates per treatment, during 10 surveys in the exposure phase (n = 30) and 6 surveys in the recovery phase (n = 18). Values for $N\text{-}NO_2^-$, $N\text{-}NH_4^+$, $N\text{-}NO_3^-$, SRP and DOC were calculated from 3 replicates per treatment during 12 surveys in the exposure phase (n = 36, except DOC where n = 30), and during 8 surveys in the recovery phase (n = 24, except DOC where n = 12).

Treatment	0%	14%	29%	43%	58%	72%	86%	100%	Recovery
pH	8.4 ± 0.1	8.4 ± 0.1	8.3 ± 0.1	8.2 ± 0.1	8.1 ± 0.1	8.0 ± 0.1	8.0 ± 0.1	7.9 ± 0.1	8.6 ± 0.0
T (°C)	21.1 ± 0.3	21.0 ± 0.2	19.4 ± 0.2	19.1 ± 0.2	19.7 ± 0.2	19.9 ± 0.2	21.0 ± 0.2	21.2 ± 0.2	20.2 ± 0.3
Conductivity ($\mu S\,cm^{-1}$)	220 ± 4	398 ± 9	584 ± 20	766 ± 28	934 ± 37	1112 ± 45	1205 ± 53	1348 ± 61	302 ± 4.3
DO ($mg\,L^{-1}$)	8.9 ± 0.1	9.0 ± 0.1	9.2 ± 0.1	8.7 ± 0.2	8.3 ± 0.3	7.8 ± 0.4	7.3 ± 0.4	6.9 ± 0.4	9.2 ± 0.1
$N\text{-}NO_2^-$ ($mg\,N\,L^{-1}$)	0.05 ± 0.0	0.4 ± 0.1	1.8 ± 0.4	2.9 ± 0.8	4.7 ± 1.2	5.5 ± 1.6	6.5 ± 2.0	5.8 ± 2.0	0.003 ± 0.0
$N\text{-}NH_4^+$ ($mg\,N\,L^{-1}$)	0.04 ± 0.02	2.0 ± 0.5	5.4 ± 1.1	7.7 ± 1.6	9.4 ± 2.1	11.8 ± 2.5	13.4 ± 2.8	16.1 ± 3.2	0.002 ± 0.0
$N\text{-}NO_3^-$ ($mg\,N\,L^{-1}$)	1.2 ± 0.0	3.7 ± 0.5	4.4 ± 0.9	6.9 ± 1.7	8.6 ± 2.3	11.9 ± 3.2	12.6 ± 3.6	16.1 ± 4.2	1.0 ± 0.1
SRP ($mg\,P\,L^{-1}$)	0.04 ± 0.03	0.03 ± 0.01	0.06 ± 0.01	0.21 ± 0.06	0.31 ± 0.09	0.44 ± 0.11	0.53 ± 0.12	0.70 ± 0.13	0.03 ± 0.01
DOC ($mg\,C\,L^{-1}$)	1.2 ± 0.1	3.0 ± 0.1	5.0 ± 0.1	7.1 ± 0.2	9.1 ± 0.3	11.3 ± 0.4	12.2 ± 0.5	14.3 ± 0.5	2.0 ± 0.0

Table 3
Linear and best-fitting model results for soluble reactive phosphorus (SRP) uptake capacity (U_{SRP}), SRP uptake efficiency (U_{SRP}/AFDM), chlorophyll-*a* (Chl-*a*), total biomass (AFDM), gross primary production (GPP), community respiration (CR) and organic matter decomposition (OMD), for immediate (measured at the end of the exposure phase) and legacy effects (measured at the end of the recovery phase). Akaike Information Criterion (AIC) and Relative Standard Errors (RSE) results are shown for the best fitted model on each case (Best fit model, Best AIC, Best RSE), but also for the simplest response, given by default in all the cases (Lin. AIC, Lin. RSE). These values verify whether the best fitted model improved the linear response results or not. Finally, pollution and legacy effects refer to whether the WWTP effluent increases (Subsidy), reduces (Stress) or produces both outcomes (Subsidy-Stress) beyond the control values (pure stream water). For more detailed information about the fitting models see Fig. 2–8, available as Supplementary material to this paper (Fig. S2–S8).

Immediate effects							
Process	U_{SRP}	U_{SRP}/AFDM	Chl-*a*	AFDM	GPP	CR	OMD
Lin. AIC	78.4	3.2	158.1	16.7	317.5	274.5	− 248.2
Lin. RSE	1.14	0.24	6.01	0.32	166.36	67.95	0.001
Best fit model	Logit	Logit	Haldane	Haldane	Quadratic	Logit	Linear
Best AIC	77.2	− 3.3	145.3	11.5	315.1	259.8	− 248.2
Best RSE	1.09	0.20	4.51	0.28	155.35	49.11	0.001
Pollution effects	**Stress**	**Stress**	**Subsidy**	**Subsidy-Stress**	**Subsidy**	**Subsidy**	**Subsidy**
Legacy effects							
Lin. AIC	59.3	− 13.3	202.6	64.3	291.4	221.4	− 258.9
Lin. RSE	0.77	0.17	15.18	0.85	96.48	22.47	0.001
Best fit model	Logit	Haldane	Quadratic	Quadratic	Quadratic	Logit	Linear
Best AIC	56.9	− 22.8	192.3	62.5	286.6	214.5	− 258.9
Best RSE	0.72	0.14	12.02	0.81	85.73	19.12	0.001
Legacy effects	**Stress**	**Subsidy-Stress**	**Subsidy**	**Subsidy-Stress**	**Subsidy**	**Subsidy**	**No legacy**

exposed to medium levels of effluent contribution ($2.9\,mg\,cm^{-2}$, 58%), being the lowest again in the most polluted treatment ($1.2\,mg\,cm^{-2}$). The data best fitted the quadratic model (Table 3, Fig. S5), thus showing similar legacy effects of subsidy-stress.

3.3. Benthic metabolism

Immediate effects of the WWTP effluent promoted GPP from 225 mg $O_2\,m^{-2}\,h^{-1}$ in the control treatment to 785 mg $O_2\,m^{-2}\,h^{-1}$ at medium levels of effluent contribution (58%), following the quadratic model (Table 3, Fig. S6). However, as values of the most polluted treatments did not fall below the control ones, it showed a saturating subsidy effect, which was most accentuated at medium concentrations and became inhibited at high levels of effluent contribution. The legacy effects followed a similar pattern (lowest production rate: 298.2 mg $O_2\,m^{-2}\,h^{-1}$, 0%; highest production rate: 499.3 mg $O_2\,m^{-2}\,h^{-1}$, 58%). Data fitted best the quadratic model (Table 3, Fig. S6), and treatments with the highest legacy did not provide values below the control ones, suggesting the same subsidy effect accentuated at medium concentrations.

Immediate effects of the WWTP effluent promoted CR from -83.8 mg $O_2\,m^{-2}\,h^{-1}$ in the control treatment to -518.4 mg $O_2\,m^{-2}\,h^{-1}$ in the most polluted, fitting a logit model which suggested a pure subsidy effect (Table 3, Fig. S7). A pollution legacy effect could also be seen by the similar pattern followed by the treatments at the end of the recovery phase (lowest oxygen consumption rate: -76.8 mg $O_2\,m^{-2}\,h^{-1}$, 0%; highest oxygen consumption rate: -183.2 mg $O_2\,m^{-2}\,h^{-1}$, 100%). Data fitted best again the logit model (Table 3, Fig. S7), indicating the same pure subsidy legacy effect.

All treatments were autotrophic. The average production-to-respiration ratio (GPP: CR) calculated for exposure and recovery phases (mean ± standard error) were of 2.17 ± 0.21 and 3.52 ± 0.30, respectively, and peaked at intermediate levels of pollution and pollution legacy (Fig. 2).

3.4. Organic matter decomposition

Immediate effects of the WWTP effluent promoted OMD to values up to $0.005\,d^{-1}$ in the most polluted treatment (Fig. 3), whereas it was lowest at medium levels of effluent contribution ($0.003\,d^{-1}$, 43%). The results best fitted a linear model (Table 3, Fig. S8), indicating a non-saturating subsidy effect on OMD. Legacy effects were weak: the slowest OMD rate ($0.011\,d^{-1}$) occurred at medium levels of effluent contribution (in the treatment 43%) and the fastest ($0.013\,d^{-1}$) in the control treatment. However, OMD fitted best a weak linear pattern (Table 3, Fig. S8), showing almost no legacy effect.

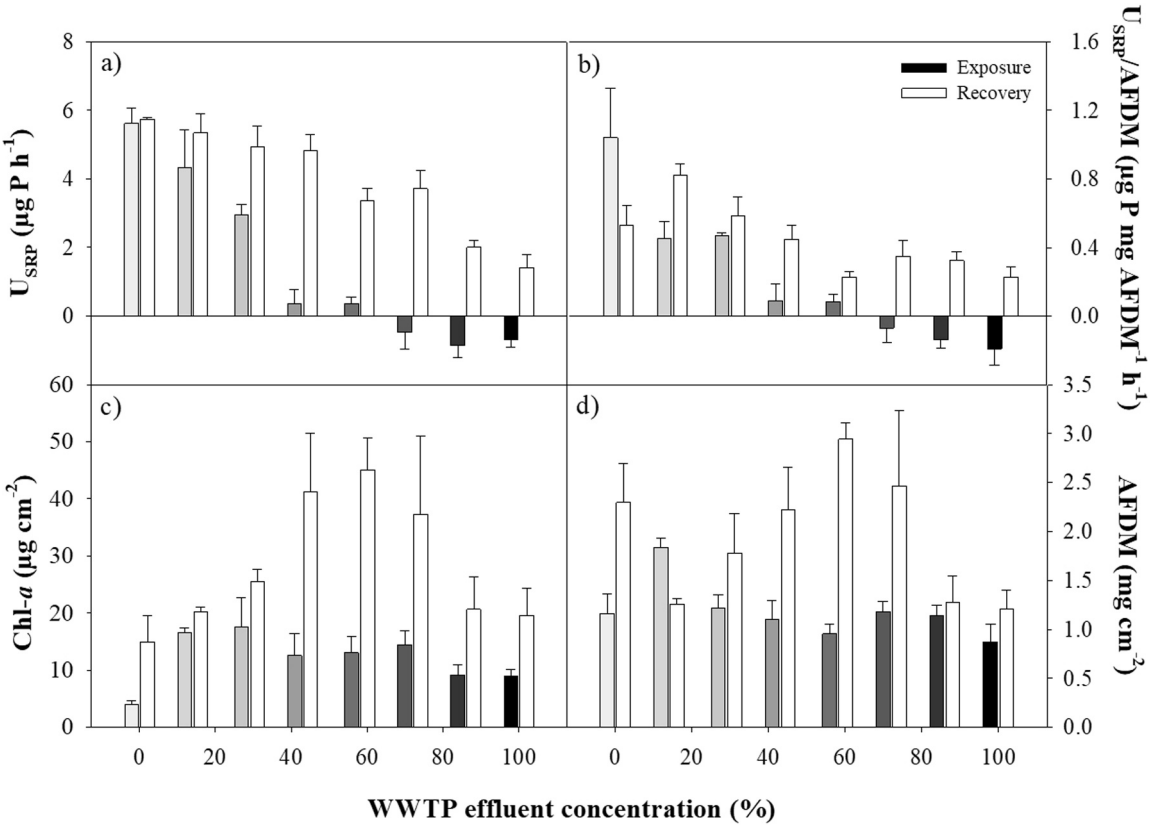

Fig. 1. Immediate (exposure phase, shaded columns) and legacy effects (recovery phase, white columns) of WWTP effluent pollution on processes measured on biofilm carriers. (a) Soluble reactive phosphorus (SRP) uptake capacity (b) SRP uptake efficiency (SRP uptake standardized by biofilm biomass), (c) chlorophyll-*a* (Chl-*a*) and (d) biofilm biomass accrual (AFDM). Values shown are mean ± standard error (SE).

4. Discussion

4.1. Ecosystem response to rising concentrations of WWTP effluents

The gradient of effluent contribution in our experiment mimicked the situation occurring in the field, where in extreme cases wastewater discharges can contribute most of the in-stream flow, transforming these streams into effluent dominated systems (Rice and Westerhoff, 2017). Despite our extreme gradient, the expected subsidy-stress scheme was only followed by biofilm biomass accrual. Otherwise, the effluent acted as a subsidy for most processes, except SRP uptake, which decreased dramatically with increasing effluent concentration. However, the patterns as well as the concentrations at which activities peaked followed process-specific responses.

Some studies (*e.g.* Clapcott et al., 2011; Woodward et al., 2012) have reported stream variables to show hump-shaped responses to stressors such as nutrient inputs, and this pattern has been often attributed to the subsidy-stress scheme described by Odum et al. (1979). Nevertheless, Odum defined stress as values of biological activity below "normal", which means that not all hump-shaped curves reflect subsidy-stress. In our case, most measured processes did not follow the subsidy-stress scheme, but were rather subsidized by the WWTP effluent, even at 100% effluent contribution. Only a few functional processes, such as the biofilm SRP uptake capacity and the biofilm biomass accrual, were reduced by the effluent, although they showed different thresholds of stress. While the biofilm SRP uptake capacity was purely stressed from the lowest levels of effluent contribution, biofilm biomass accrual followed the subsidy-stress pattern, shifting from being subsidized to be stressed at medium levels of effluent contribution. These results show that, despite the presence of toxic compounds, the main overall effect of the complex mixture of substances in the WWTP effluent used in the present experiment was to subsidize biological activity.

According to the EU-funded ENERWATER research project (http://www.enerwater.eu/), the effluents from WWTPs worldwide span a very large range of nutrient concentration (0.1–95 mg N L^{-1} and 0.1–9 mg P L^{-1} for total nitrogen and total phosphorus, respectively) (ENERWATER, 2018). Our effluent fits in the low range of both nutrients, meaning that more stress responses could have been detected with effluents fitting higher ranges of nutrient concentrations. Regarding heavy metals, the most abundant in our effluent were copper and zinc, which are among the top five metals of concern in freshwater ecosystems (Su et al., 2017). Clements et al. (1992) showed a reduction in benthic invertebrates after 10 d of exposure to 25 µg L^{-1} of copper, which was followed by a shift in community composition from sensitive to tolerant taxa. Similarly, Wong and Chau (1990) found toxic effects for freshwater algae after exposure to 30 µg L^{-1} of zinc. In our experiment, these concentrations were exceeded by far (82 µg Cu L^{-1} and 72 µg Zn L^{-1}), which suggests there were toxic effects for the biological communities in some of our artificial streams. However, most of the measured functional processes were not inhibited, which suggests that the biofilm community was evolving towards a more resistant community (Niyogi et al., 2002; Costello et al., 2016).

The response of some of the functional processes measured (quadratic for GPP, logit for CR and linear for OMD) best fitted models indicating that the effluent produced a non-saturating subsidy effect. In those cases, the potential toxic effects of the effluent were upset by factors promoting biological activity, which seemed not to be limiting. Probably, the high nutrient supply (up to 400-fold times higher than in the control), the absence of light limitation and the warm water temperature in our experiment promoted these microbially-mediated processes, as has been shown in open streams placed below WWTP effluents (Stelzer et al., 2003; Albek, 2003; von Schiller et al., 2007).

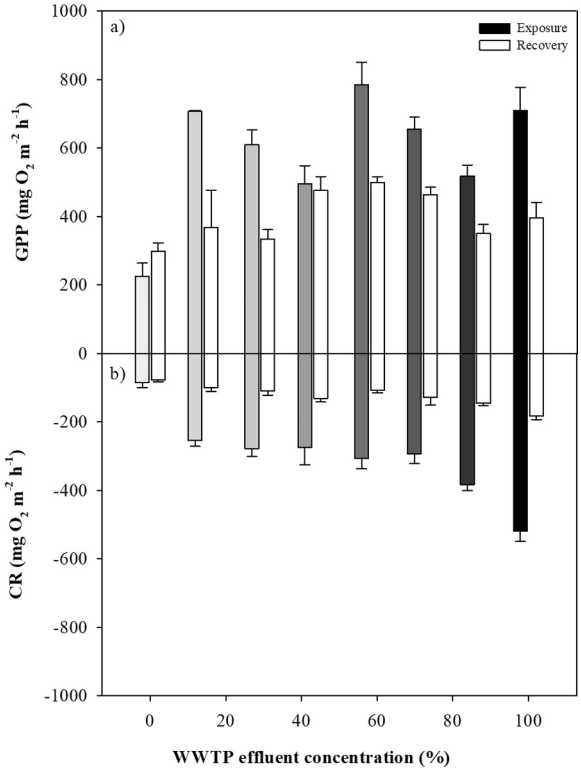

Fig. 2. Immediate (exposure phase, shaded columns) and legacy effects (recovery phase, white columns) of WWTP effluent pollution on benthic metabolism. (a) Gross primary production (GPP) and (b) Community respiration (CR) measured on epipsammic and epilithic biofilm. Values shown are mean ± standard error (SE).

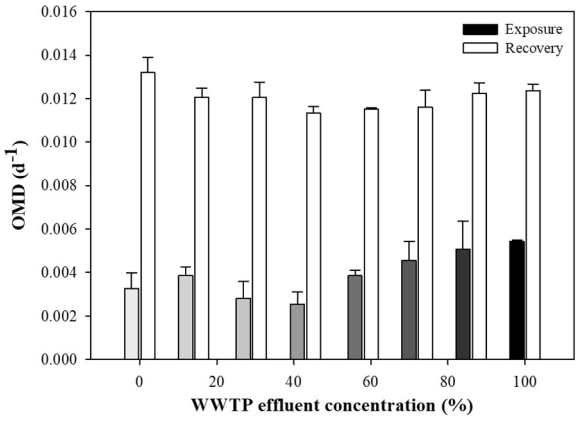

Fig. 3. Immediate (exposure phase, shaded columns) and legacy effects (recovery phase, white columns) of WWTP effluent pollution on organic matter decomposition (OMD). Values shown are mean ± standard error (SE).

These results are in line with previous studies where high nutrient concentrations and warm water temperatures were reported as the main drivers of faster decomposition rates in effluent-dominated streams (Spänhoff et al., 2007). Still, we expected that the high concentrations of both assimilable and toxic compounds in the most concentrated treatments would produce stress effects and limit processing rates, but this was not the case. Our results for benthic metabolism also support that the higher nutrient concentrations derived from wastewater effluents would promote overall ecosystem metabolism (Gücker et al., 2006; Izagirre et al., 2008). At medium pollution levels, however, primary production became saturated while respiration increased dramatically. After 15 d of exposure to the WWTP effluent, some of the most polluted treatments started to show hypoxic conditions during the night (DO concentrations down to 4 mg L^{-1}), and reached anoxic conditions (1 mg L^{-1}) after 25 d of exposure. Overall, these are signals of eutrophication in the most polluted treatments (Smith, 2003; Brack et al., 2007).

Some other response models (Haldane for Chl-*a* and AFDM) indicate that the effluent produced a saturating subsidy effect on these processes, with inhibition at higher levels of effluent contribution. Medium pollution concentrations were saturating for both processes and the highest pollution levels induced inhibition, and even stress in the case of biofilm biomass. This saturating subsidy effect has been widely described in the literature (Paul and Meyer, 2001), together with the toxic effects that could be produced by higher nutrient concentrations (Ribot et al., 2015). Interestingly, this saturation threshold was achieved at lower levels of effluent contribution for both Chl-*a* and AFDM than for GPP, suggesting that structural variables could be more sensitive than those related to ecosystem functioning. However, the decreasing tendencies caused by inhibition at higher levels of effluent contribution did not fit the non-saturating tendencies observed for both OMD and CR. This suggests that effects can depend on the type of organism. It is well known that nutrient inputs below WWTP effluents may induce changes in species composition (Bernhardt and Likens, 2004; Domingues et al., 2011; Drury et al., 2013), and this could affect both the primary producers as well as the heterotrophs existing in our artificial streams, which could have favoured the presence of a more homogeneous but resistant community.

Finally, the logit model showed that the effluent had a pure stress effect on SRP uptake capacity and efficiency, as both activities decreased since the lowest levels of pollution. The demand for nutrients dissolved in the water column is affected by the balance between the biofilm and the water column, and thus internal recycling gains importance when the external supply is comparatively low (Mulholland, 1996; Hall et al., 2002). Under high external nutrient supply, biofilms become less efficient in nutrient removal from the water column (Martí et al., 2004; Proia et al., 2017), to the most extreme cases where no nutrient removal occurs due to a saturation of the system (Earl et al., 2006). Moreover, in our experiment, SRP concentrations in the most polluted treatments were higher than in the bioassay standard solution, which could have led to abiotic desorption of SRP by the biofilms. Therefore, our results point to a combination of biotic saturation of SRP removal and shifts in abiotic sorption-desorption mechanisms as the main causes of the observed decline in SRP uptake capacity and efficiency along the gradient of increasing pollution contribution.

4.2. Legacy effects

Most measured processes showed clear legacy effects of pollution, despite a higher biological activity at the end of the recovery phase than at the end of the exposure phase. However, these legacy effects followed either subsidy, stress, or subsidy-stress dynamics.

For most of the processes, the response model for the legacy effect was the same as for the immediate effect despite the inclusion of colonized cobbles from the unpolluted Llémena River at the onset of the recovery phase. This fact suggests that the biofilm community in the channels had acquired some degree of resistance to the new inoculum. During the whole experiment, the water flow was slow, which has been shown to enhance biofilm biomass, thickness and complexity (Battin et al., 2003). These thick biofilm structures reduce the hydraulic exchange between the biofilm and the water column, promoting internal cycling processes (Earl et al., 2006; Johnson et al., 2015). Thus, thick biofilm can store large concentrations of nutrients, as we observed in the experiment even weeks after the effluent flow ceased. The storage of nutrients and other pollutants within the biofilm could be the main cause for the persistence of the similar subsidy, stress or subsidy-stress patterns for immediate and legacy responses. Results found in another add-on work to this experiment (Vicenç Acuña, *Unpublished data*)

support this idea, as they found phosphate desorption from the sediment and biofilm during the recovery phase.

Most studies assessing the effects of urban pollution on stream ecosystem functioning are usually based on the comparison between reaches located upstream and downstream from existing point-source inputs (*e.g.*, Sánchez-Pérez et al., 2009). Although field studies offer greater realism than laboratory experiments, the latter offer the opportunity to ask questions impossible to answer with just observational studies, such as the effect of the dilution rate of WWTP effluents.

5. Conclusions

Urban pollution from WWTPs affected the functioning of our mesocosm ecosystems, although mostly not following the subsidy-stress scheme we expected. Instead, subsidy responses were prevalent among the variables measured, even though complex and process-specific patterns were observed. Legacy effects occurred for most of the studied processes and followed a similar pattern to that of immediate effects, although responses became more complex, mainly driven by the internal cycling occurring within biofilms. Overall, the effluent used in the present experiment produced complex effects, and we could, thus suspect even more complex responses in real-world freshwater ecosystems.

Acknowledgments

This research was supported by the European Union 7th Framework Programme (GLOBAQUA; 603629-ENV-2013-6.2.1). Authors also acknowledge the financial support from the University of the Basque Country (pre-doctoral fellowship to O. Pereda), the Basque Government (Consolidated Research Group: Stream Ecology 7-CA-18/10), and the Economy and Knowledge Department of the Catalan Government (Consolidated Research Group: ICRA-ENV 2017 SGR 1124). Authors are also especially grateful to Maria Casellas, Carme Font, Carmen Gutiérrez, Ferran Romero and Laia Sabater-Liesa for their assistance during the laboratory experiments.

Appendix A. Supporting information

Supplementary data associated with this article can be found in the online version at doi:10.1016/j.ecoenv.2018.11.103.

References

Acuña, V., Wolf, A., Uehlinger, U., Tockner, K., 2008. Temperature dependence of stream benthic respiration in an Alpine river network under global warming. Freshw. Biol. 53, 2076–2088. https://doi.org/10.1111/j.1365-2427.2008.02028.x.

Acuña, V., Casellas, M., Corcoll, N., Timoner, X., Sabater, S., 2015. Increasing extent of periods of no flow in intermittent waterways promotes heterotrophy. Freshw. Biol. 60 (9), 1810–1823. https://doi.org/10.1111/fwb.12612.

Albek, E., 2003. Estimation of point and diffuse contaminant loads to streams by non-parametric regressions analysis monitoring data. Water Air Soil Pollut. 147, 229–243. https://doi.org/10.1023/A:1024592815576.

Alvarez, D., Perkins, S., Nilsen, E., Morace, J., 2014. Spatial and temporal trends in occurrence of emerging and legacy contaminants in the Lower Columbia River 2008–2010. Sci. Total Environ. 484, 322–330. https://doi.org/10.1016/j.scitotenv.2013.07.128.

Aristi, I., von Schiller, D., Arroita, M., Barceló, D., Ponsatí, L., García-Galán, M.J., Sabater, S., Elosegi, A., Acuña, V., 2015. Mixed effects of effluents from a wastewater treatment plant on river ecosystem metabolism: subsidy or stress? Freshw. Biol. 60, 1398–1410. https://doi.org/10.1111/fwb.12576.

Aristi, I., Casellas, M., Elosegi, A., Insa, S., Petrovic, M., Sabater, S., Acuña, V., 2016. Nutrients versus emerging contaminants – or a dynamic match between subsidy and stress effects on stream biofilms? Environ. Pollut. 212, 208–215. https://doi.org/10.1016/j.envpol.2016.01.067.

Arroita, M., Flores, L., Larrañaga, A., Martínez, A., Martínez-Santos, M., Pereda, O., Ruiz-Somera, E., Solagaistua, L., Elosegi, A., 2016. Water abstraction impacts stream ecosystem functioning via wetted-channel contraction. Freshw. Biol. 62 (2), 243–257. https://doi.org/10.1111/fwb.12864.

Austin, M.P., 2002. Spatial prediction of species distribution: an interface between ecological theory and statistical modeling. Ecol. Model. 157, 101–118. https://doi.org/10.1016/S0304-3800(02)00205-3.

Aymerich, I., Acuña, V., Ort, C., Rodríguez-Roda, I., Corominas, Ll, 2017. Fate or organic microcontaminants in wastewater treatment and river systems: an uncertainty assessment in view of sampling strategy, and compound consumption rate and degradability. Water Res. 125, 152–161. https://doi.org/10.1016/j.watres.2017.08.011.

Baldwin, D.S., Rees, G.N., Edwards, M., Robertson, A.I., 2003. A simple, reproducible substrate for studying biofilms in aquatic environments. Environ. Technol. 24 (6), 711–717. https://doi.org/10.1080/09593330309385607.

Battin, T.J., Kaplan, L.A., Newbold, J.D., Hansen, C.M.E., 2003. Contributions of microbial biofilms to ecosystem processes in stream mesocosms. Nature 426, 439–442. https://doi.org/10.1038/nature02152.

Benton, T.G., Solan, M., Travis, J.M.J., Sait, S.M., 2007. Microcosm experiments can inform global ecological problems. Trends Ecol. Evol. 22 (10), 516–521. https://doi.org/10.1016/j.tree.2007.08.003.

Bernhardt, E.S., Likens, G.E., 2004. Controls on periphyton biomass in heterotrophic streams. Freshw. Biol. 49, 14–27. https://doi.org/10.1046/j.1365-2426.2003.01161.x.

Beyene, A., Legesse, W., Triest, L., Kloos, H., 2009. Urban impact on ecological integrity of nearby rivers in developing countries: the Borkena River in highland Ethiopia. Environ. Monit. Assess. 153, 461–476. https://doi.org/10.1007/s10661-008-0371-x.

Birk, S., Bonne, W., Borja, A., Brucet, S., Courrat, A., Poikane, S., Solimini, A., van de Bund, W., Zampoukas, N., Hering, D., 2012. Three hundred ways to assess Europe's surface waters: an almost complete overview of biological methods to implement the Water Framework Directive. Ecol. Indic. 18, 31–41. https://doi.org/10.1016/j.ecolind.2011.10.009.

Bonnineau, C., Guasch, H., Proia, L., Ricart, M., Geiszinger, A., Romaní, A.M., Sabater, S., 2010. Fluvial biofilms: a pertinent tool to assess β-blockers toxicity. Aquat. Toxicol. 96 (3), 225–233. https://doi.org/10.1016/j.aquatox.2009.10.024.

Brack, W., Klamer, H.J.C., López de Alda, M., Barceló, D., 2007. Effect-directed analysis of key toxicants in European river basins. A review. Environ. Sci. Pollut. Res. 14, 30–38. https://doi.org/10.1065/espr2006.08.329.

Bundschuh, M., Pierstorf, R., Schreiber, W.H., Schulz, R., 2011. Positive effects of wastewater ozonation displayed by *in situ* bioassays in the receiving stream. Environ. Sci. Technol. 45 (8), 3774–3780. https://doi.org/10.1021/es104195h.

Camargo, J.A., Alonso, A., 2006. Ecological and toxicological effects of inorganic nitrogen pollution in aquatic ecosystems: a global assessment. Environ. Int. 32, 831–849. https://doi.org/10.1016/j.envint.2006.05.002.

Cardinale, B.J., Bier, R., Kwan, C., 2012. Effects of TiO_2 nanoparticles on the growth and metabolism of three species of freshwater algae. J. Nanopart. Res. 14, 913. https://doi.org/10.1007/s11051-012-0913-6.

Carey, R.O., Migliaccio, K.W., 2009. Contribution of wastewater treatment plant effluents to nutrient dynamics in aquatic systems: a review. Environ. Manag. 44 (2), 205–217. https://doi.org/10.1007/s00267-009-9309-5.

Carl, G., Kühn, I., 2007. Analyzing spatial autocorrelation in species distributions using Gaussian and logit models. Ecol. Model. 207, 159–170. https://doi.org/10.1016/j.ecolmodel.2007.04.024.

Chambers, J.M., 1992. Linear Models. In: Chambers, J.M., Hastie, T.J. (Eds.), Chapter 4 of Statistical Models in S. Wadsworth & Brooks/Cole (ISBN: 0534167659, 9780534167653).

Clapcott, J., Young, R., Goodwin, E., Leathwick, J., Kelly, D., 2011. Relationships between multiple land-use pressures and individual and combined indicators of stream ecological integrity. DOC Research and Development Series 365 NZ Department of Conservation, Wellington, New Zealand (ISBN: 978-0-478-14915-9).

Clements, W.H., Cherry, D.S., van Hassel, J.H., 1992. Assessment of the impact of heavy metals on benthic communities at the Clinch River (Virginia): evaluation of an Index of Community Sensitivity. Can. J. Fish. Aquat. Sci. 49 (8), 1686–1694. https://doi.org/10.1139/f92-187.

Corcoll, N., Casellas, M., Huerta, B., Guasch, H., Acuña, V., Rodríguez-Mozaz, S., Serra-Compte, A., Barceló, D., Sabater, S., 2015. Effects of flow intermittency and pharmaceutical exposure on the structure and metabolism of stream biofilms. Sci. Total Environ. 503–504, 159–170. https://doi.org/10.1016/j.scitotenv.2014.06.093.

Costello, D.M., Rosi-Marshall, E.J., Shaw, L.E., Grace, M.R., Kelly, J.J., 2016. A novel method to assess effects of chemical stressors on natural biofilm structure and function. Freshw. Biol. 61, 2129–2140. https://doi.org/10.1111/fwb.12641.

Domingues, R.B., Barbosa, A.B., Sommer, U., Galvao, H.M., 2011. Ammonium, nitrate and phytoplankton interactions in a freshwater tidal estuarine zone: potential effects of cultural eutrophication. Aquat. Sci. 73, 331–343. https://doi.org/10.1007/s00027-011-0180-0.

Drury, B., Rosi-Marshall, E., Kelly, J.J., 2013. Wastewater treatment effluent reduces the abundance and diversity of benthic bacterial communities in urban and suburban rivers. Appl. Environ. Microbiol. 79 (6), 1897–1905. https://doi.org/10.1128/AEM.03527-12.

Earl, S.R., Valett, H.M., Webster, J.R., 2006. Nitrogen saturation in stream ecosystems. Ecology 87, 3140–3151. https://doi.org/10.1890/0012-9658(2006)87[3140:NSISE]2.0.CO;2.

Elosegi, A., Nicolás, A., Richardson, J.S., 2018. Priming of leaf litter decomposition by algae seems of minor importance in natural streams during autumn. PLoS One 13 (9), e0200180. https://doi.org/10.1371/journal.pone.0200180.

ENERWATER Benchmarking Database. 〈http://www.enerwater.eu/energy-benchmarking-database/〉 (Accessed 6 August 2018).

Englert, D., Zubrod, J.P., Schulz, R., Bundschuh, M., 2013. Effects of municipal wastewater on aquatic ecosystem structure and function in the receiving stream. Sci. Total Environ. 454–455, 401–410. https://doi.org/10.1016/j.scitotenv.2013.03.025.

Freixa, A., Acuña, V., Casellas, M., Pecheva, S., Romaní, A.M., 2017. Warmer night-time temperature promotes microbial heterotrophic activity and modifies stream sediment community. Glob. Change Biol. 23 (9), 3825–3837. https://doi.org/10.1111/gcb.

13664.
Gros, M., Petrovic, M., Barceló, D., 2007. Wastewater treatment plants as a pathway for aquatic contamination by pharmaceuticals in the Ebro River basin (Northeast Spain). Environ. Toxicol. Chem. 26 (8), 1553–1562. https://doi.org/10.1897/06-495R.1.
Gücker, B., Brauns, M., Pusch, M.T., 2006. Effects of wastewater treatment plant discharge on ecosystem structure and function of lowland streams. J. N. Am. Benthol. Soc. 25 (2), 313–329. https://doi.org/10.1899/0887-3593(2006)25[313:eowtpd]2.0.co;2.
Haggard, B.E., Storm, D.E., Stanley, E.H., 2001. Effect of a point source input on stream nutrient retention. J. Am. Water Resour. Assoc. 37 (5), 1291–1299. https://doi.org/10.1111/j.1752-1688.2001.tb03639.x.
Haggard, B.E., Stanley, E.H., Storm, D.E., 2005. Nutrient retention in a point-source-enriched stream. J. N. Am. Benthol. Soc. 24 (1), 29–47. https://doi.org/10.1899/0887-3593(2005)024<0029:NRIAPS>2.0.CO;2.
Haldane, J.B.S., 1930. Enzymes. J. Chem. Technol. Biotechnol. 919–920. https://doi.org/10.1002/jctb.5000494433.
Hall, R.O., Bernhardt, E.S., Likens, G.E., 2002. Relating nutrient uptake with transient storage in forested mountain streams. Limnol. Oceanogr. 47 (1), 255–265. https://doi.org/10.4319/lo.2002.47.1.0255.
Hanley, N., Wright, R.E., Adamowicz, V., 1998. Using choice experiments to value the environment. Environ. Resour. Econ. 11 (3–4), 413–428. https://doi.org/10.1023/A:1008287310583.
Hisdal, H., Stahl, K., Tallaksen, L.M., Demuth, S., 2001. Have streamflow droughts in Europe become more severe or frequent? Int. J. Climatol. 21, 317–333. https://doi.org/10.1002/joc.619.
Holeton, C., Chambers, P.A., Grace, L., 2011. Wastewater release and its impacts on Canadian waters. Can. J. Fish. Aquat. Sci. 68 (10), 1836–1859. https://doi.org/10.1139/f2011-096.
Hoppe, P.D., Rosi-Marshall, E.J., Bechtold, H.A., 2012. The antihistamine cimetidine alters invertebrate growth and population dynamics in artificial streams. Freshw. Sci. 31 (2), 379–388. https://doi.org/10.1899/11-089.
Izagirre, O., Agirre, U., Bermejo, M., Pozo, J., Elosegi, A., 2008. Environmental controls of whole-stream metabolism identified from continuous monitoring of Basque streams. J. N. Am. Benthol. Soc. 27 (2), 252–268. https://doi.org/10.1899/07-022.1.
Jeffrey, S., Humphrey, G., 1975. New spectrophotometric equations for determining chlorophylls a, b, c1 and c2 in higher-plants, algae and natural phytoplankton. Biochem. Physiol. Pflanz. 167, 191–194. https://doi.org/10.1016/S0015-3796(17)30778-3.
Johnson, Z.C., Warwick, J.J., Schumer, R., 2015. Nitrogen retention in the main channel and two transient storage zones during nutrient addition experiments. Limnol. Oceanogr. 60, 57–77. https://doi.org/10.1002/lno.10006.
Jones, B., O'Neill, B.C., 2016. Spatially explicit global population scenarios consistent with the Shared Socioeconomic Pathways. Environ. Res. Lett. 11, 084003. https://doi.org/10.1088/1748-9326/11/8/084003.
Lee, S.S., Paspalof, A.M., Snow, D.D., Richmond, E.K., Rosi-Marshall, E.J., Kelly, J.J., 2016. Occurrence and potential biological effects of amphetamine on stream communities. Environ. Sci. Technol. 50 (17), 9727–9735. https://doi.org/10.1021/acs.est.6b03717.
Marquet, P.A., Quiñones, R.A., Abades, S., Labra, F., Tognelli, M., Arim, M., Rivadeneira, M., 2005. Review: scaling and power-laws in ecological systems. J. Exp. Biol. 208, 1749–1769. https://doi.org/10.1242/jeb.01588.
Martí, E., Aumatell, J., Godé, L., Poch, M., Sabater, F., 2004. Nutrient retention efficiency in streams receiving inputs from wastewater treatment plants. J. Environ. Qual. 33, 285–293. https://doi.org/10.2134/jeq. 2004.0285.
Martí, E., Riera, J.L., Sabater, F., 2009. Effects of wastewater treatment plants on stream nutrient dynamics under water scarcity conditions. In: Sabater, S., Barceló, D. (Eds.), Water Scarcity in the Mediterranean. The Handbook of Environmental Chemistry 8. Springer, Berlin, Heidelberg, pp. 173–195. https://doi.org/10.1007/698_2009_33.
McFadden, D., 1974. Conditional logit analysis of qualitative choice behavior. In: Zarembka, P. (Ed.), Frontiers in Econometrics. Academic Press, New York.
Merseburger, G.C., Martí, E., Sabater, F., 2005. Net changes in nutrient concentrations below a point source input in two streams draining catchments with contrasting land uses. Sci. Total Environ. 347, 217–229. https://doi.org/10.1016/j.scitotenv.2004.12.022.
Merseburger, G.C., Martí, E., Sabater, F., Ortiz, J.D., 2011. Point-source effects on N and P uptake in a forested and an agricultural Mediterranean streams. Sci. Total Environ. 409, 957–967. https://doi.org/10.1016/j.scitotenv.2010.11.014.
Millennium Ecosystem Assessment, 2005. Ecosystems and Human Well-Being: Biodiversity Synthesis. World Resources Institute.
Mogens, H., Gujer, W., Mino, T., van Loosdrecht, M., 2000. Activated Sludge Models ASM1, ASM2, ASM2d and ASM3. IAWPRC Scientific and Technical Reports, 9. IWA Publishing, London, U.K (ISBN: 9781780402369).
Monod, J., 1949. The growth of bacterial cultures. Annu. Rev. Microbiol. 3, 371–394. https://doi.org/10.1146/annurev.mi.03.100149.002103.
Mulholland, P.J., 1996. Role in nutrient cycling in streams. In: Stevenson, R.J., Bothwell, M.L., Lowe, R.L. (Eds.), Algal Ecology. Academic Press, California, pp. 609–639 (ISBN: 9780080526942).
Murphy, J., Riley, J.P., 1962. A modified single solution method for the determination of phosphate in natural waters. Anal. Chim. Acta 27, 31–36. https://doi.org/10.1016/S0003-2670(00)88444-5.
Navarro, E., Guasch, H., Muñoz, I., Real, M., Sabater, S., 2000. Aplicación de un sistema de canales artificiales en el estudio ecotoxicológico de comunidades microbentónicas. Limnetica 18, 1–14.
Niyogi, D.K., Lewis, W.M., McKnight, D.M., 2002. Effects of stress from mine drainage on diversity, biomass and function of primary producers in mountain streams. Ecosystems 5 (6), 554–567. https://doi.org/10.1007/s10021-002-0182-9.
Odum, E.P., Finn, J.T., Franz, E.H., 1979. Perturbation theory and the subsidy-stress gradient. Bioscience 29, 349–352. https://doi.org/10.2307/1307690.
Otto, S.P., Day, T., 2007. A Biologist's Guide to Mathematical Modeling in Ecology and Evolution. Princeton University Press (744 pp. ISBN: 9780691123448).
Pascoal, C., Pinho, M., Cássio, F., Gomes, P., 2003. Assessing structural and functional ecosystem condition using leaf breakdown: studies on a polluted river. Freshw. Biol. 48, 2033–2044. https://doi.org/10.1046/j.1365-2427.2003.01130.x.
Paul, M.J., Meyer, J.L., 2001. Streams in the urban landscape. Annu. Rev. Ecol. Syst. 32, 333–365. https://doi.org/10.1146/annurev.ecolsys.32.081501.114040.
Peters, R.H., 1983. The Ecological Implications of Body Size. Cambridge University Press, Cambridge, U.K.. https://doi.org/10.1017/CBO9780511608551.
Peters, K., Bundschuh, M., Schäfer, R.B., 2013. Review on the effects of toxicants on freshwater ecosystem functions. Environ. Pollut. 180, 324–329. https://doi.org/10.1016/j.envpol.2013.05.025.
Petersen, R.C., Cummins, K.W., 1974. Leaf processing in a woodland stream. Freshw. Biol. 4, 345–368. https://doi.org/10.1111/j.1365-2427.1974.tb00103.x.
Pinheiro J., Bates D., DebRoy S., Sarkar D., Core Team, R., 2018. nlme: Linear and Nonlinear Mixed Effects Models. R package version 3.1.-131. 〈https://CRAN.R-project.org/package=nlme〉.
Proia, L., Romaní, A., Sabater, S., 2017. Biofilm phosphorus uptake capacity as a tool for the assessment of pollutant effects in river ecosystems. Ecotoxicology 26 (2), 271–282. https://doi.org/10.1007/s10646-017-1761-z.
R Core Team, 2017. R: a language and environment for statistical computing. R Foundation for Statistical Computing, Vienna, Austria (URL). 〈https://www.R-project.org〉.
Ribot, M., Martí, E., von Schiller, D., Sabater, F., Daims, H., Battin, T.J., 2012. Nitrogen processing and the role of epilithic biofilms downstream of a wastwater treatment plant. Freshw. Sci. 31, 1057–1069. https://doi.org/10.1899/11-161.1.
Ribot, M., von Schiller, D., Sabater, F., Martí, E., 2015. Biofilm growth and nitrogen uptake responses to increases in nitrate and ammonium availability. Aquat. Sci. 77 (4), 695–707. https://doi.org/10.1007/s00027-015-0412-9.
Rice, J., Westerhoff, P., 2017. High levels of endocrine pollutants in US streams during low flow due to insufficient wastewater dilution. Nat. Geosci. 10, 587–591. https://doi.org/10.1038/ngeo2984.
Ricklefs, R.E., 1967. A graphical method of fitting equations to growth curves. Ecology 48 (6), 978–983. https://doi.org/10.2307/1934545.
Rodríguez-Mozaz, S., Weinberg, H.S., 2010. Meeting report: pharmaceuticals in water – an interdisciplinary approach to a public health challenge. Environ. Health Perspect. 118, 1016–1020. https://doi.org/10.1289/ehp.0901532.
Rosi-Marshall, E.J., Snow, D., Bartelt-Hunt, S.L., Paspalof, A., Tank, J.L., 2015. A review of ecological effects and environmental fate of illicit drugs in aquatic ecosystems. J. Hazard. Mater. 282, 18–25. https://doi.org/10.1016/j.jhazmat.2014.06.062.
Sánchez-Pérez, J.M., Gerino, M., Sauvage, S., Dumas, P., Maneux, É., Julien, F., Winterton, P., Vervier, P., 2009. Effects of wastewater treatment plant pollution on in-stream ecosystems functions in an agricultural watershed. Ann. Limnol. – Int. J. Limnol. 45, 79–92. https://doi.org/10.1051/limn/2009011.
Santos, L.H.M.L.M., Gros, M., Rodriguez-Mozaz, S., Delerue-Matos, C., Pena, A., Barceló, D., Montenegro, M.C.B.S.M., 2013. Contribution of hospital effluents to the load of pharmaceuticals in urban wastewaters: identification of ecologically relevant pharmaceuticals. Sci. Total Environ. 461–462, 302–316. https://doi.org/10.1016/j.scitotenv.2013.04.077.
Segner, H., Schmitt-Jansen, M., Sabater, S., 2014. Assessing the impact of multiple stressors on aquatic biota: the receptor´s side matters. Environ. Sci. Technol. 48, 7690–7696. https://doi.org/10.1021/es405082t.
Serra, A., Guasch, H., Admiraal, W., Van der Geest, H.G., Van Beusekom, S.A.M., 2010. Influence of phosphorus on copper sensitivity of fluvial periphyton: the role of chemical, physiological and community-related factors. Ecotoxicology 19 (4), 770–780. https://doi.org/10.1007/s10646-009-0454-7.
Serrano, A., 2007. Plan Nacional de Calidad de las aguas 2007–2015. Ambienta 69, 6–13.
Sharpley, A., Jarvie, H.P., Buda, A., May, L., Spears, B., Kleinman, P., 2013. Phosphorus legacy: overcoming the effects of past management practices to mitigate future water quality impairment. J. Environ. Qual. 42 (5), 1308–1326. https://doi.org/10.2134/jeq.2013.03.0098.
Smith, V.H., 2003. Eutrophication of freshwater and coastal marine ecosystems a global problem. Environ. Sci. Pollut. Res. 10, 126–139. https://doi.org/10.1065/espr2002.12.142.
Spänhoff, B., Bischof, R., Böhme, A., Lorenz, S., Neumeister, K., Nöthlich, A., Küsel, K., 2007. Assessing the impact of effluents from a modern waste water treatment plan on breakdown of coarse particulate organic matter and benthic macroinvertebrates in a lowland river. Water Air Soil Pollut. 180, 119–129. https://doi.org/10.1007/s11270-006-9255-2.
Steinman, A.D., Lamberti, G.A., Leavitt, P.R., 2006. Biomass and pigments of benthic algae. In: Hauer, F.R., Lamberti, G.A. (Eds.), Methods in Stream Ecology. Academic Press, San Diego, pp. 357–379. https://doi.org/10.1016/B978-012332908-0.50024-3.
Su, C., Lu, Y., Johnson, A.C., Shi, Y., Zhang, M., Zhang, Y., Juergens, M.D., Jin, X., 2017. Which metal represents the greatest risk to freshwater ecosystem in Bohai Region of China? Ecosyst. Health Sustain. 3 (2), e01260. https://doi.org/10.1002/ehs2.1260.
Subirats, J., Timoner, X., Sànchez-Melsió, A., Balcázar, J.L., Acuña, V., Sabater, S., Borrego, C., 2018. Emerging contaminants and nutrients synergistically affect the spread of class 1 integron-integrase (intI1) amdsul1 genes within stable streambed bacterial communities. Water Res. 138, 77–85. https://doi.org/10.1016/j.watres.2018.03.025.
Stelzer, R.S., Heffernan, J., Likens, G.E., 2003. The influence of dissolved nutrients and particulate organic matter quality on microbial respiration and biomass in a forest stream. Freshw. Biol. 48, 1925–1937. https://doi.org/10.1046/j.1365-2427.2003.

01141.x.
von Schiller, D., Martí, E., Riera, J.L., Sabater, F., 2007. Effects of nutrients and light on periphyton biomass and nitrogen uptake in Mediterranean streams with contrasting land uses. Freshw. Biol. 52, 891–906. https://doi.org/10.1111/j.1365-2427.2007.01742.x.
von Schiller, D., Acuña, V., Aristi, I., Arroita, M., Basaguren, A., Bellin, A., Boyero, L., Butturini, A., Ginebreda, A., Kalogianni, E., Larrañaga, A., Majone, B., Martínez, A., Monroy, S., Muñoz, I., Paunović, M., Pereda, O., Petrovic, M., Pozo, J., Rodríguez-Mozaz, S., Rivas, D., Sabater, S., Sabater, F., Skoulikidis, N., Solagaistua, L., Vardakas, L., Elosegi, A., 2017. River ecosystem processes: a synthesis of approaches, criteria of use and sensitivity to environmental stressors. Sci. Total Environ. 596–597, 465–480. https://doi.org/10.1016/j.scitotenv.2017.04.081.
Tchobanoglous, G., Burton, F.L., 1991. Wastewater engineering: treatments, disposal and reuse. Series in Water Resources and Environmental Engineering, 3rd edition. McGraw-Hill, New York (ISBN: 978-0070416901).
Tilman, D., Isbell, F., Cowles, J.M., 2014. Biodiversity and ecosystem functioning. Annu. Rev. Ecol. Evol. Syst. 45, 471–493. https://doi.org/10.1146/annurev-ecolsys-120213-091917.
Vandermeer, J., 2010. How populations grow: the exponential and logistic equations. Nat. Educ. Knowl. 3 (10), 15.
Vörösmarty, C.J., McIntyre, P.B., Gessner, M.O., Dudgeon, D., Prusevich, A., Green, P., Glidden, S., Bun, S.E., Sullivan, C.A., Reidy Liermann, C., Davies, P.M., 2010. Global threats to human water security and river biodiversity. Nature 467, 555–561. https://doi.org/10.1038/nature09440.
Wagenhoff, A., Townsend, C.R., Phillips, N., Matthaei, C.D., 2011. Subsidy-Stress and multiple-stressor effects along gradients of deposited fine sediment and dissolved nutrients in a regional set of streams and rivers. Freshw. Biol. 56, 1916–1936. https://doi.org/10.1111/j.1365-2427.2011.02619.x.
Wagenhoff, A., Townsend, C.R., Matthaei, C.D., 2012. Macroinvertebrate responses along broad stressor gradients of deposited fine sediment and dissolved nutrients: a stream mesocosm experiment. J. Appl. Ecol. 49, 892–902. https://doi.org/10.1111/j.1365-2664.2012.02162.x.
Wagenhoff, A., Lange, K., Townsend, C.R., Matthaei, C.D., 2013. Patterns of benthic algae and cyanobacteria along twin-stressor gradients of nutrient and fine sediment: a stream mesocosm experiment. Freshw. Biol. 58, 1849–1863. https://doi.org/10.1111/fwb.12174.
Weir, I.S., Pettit, A.N., 2000. Binary probability maps using a hidden conditional autoregressive Gaussian process with an application to Finnish common toad data. J. Appl. Stat. 49 (473), 484. https://doi.org/10.1111/1467-9876.00206.
Wong, P.T.S., Chau, Y.K., 1990. Zinc toxicity to freshwater algae. Toxic. Assess. 5 (2), 167–177. https://doi.org/10.1002/tox.2540050205.
Woodward, G., Gessner, M.O., Giller, P.S., Gulis, V., Hladyz, S., Lecerf, A., Malmqvist, B., Mckie, B.G., Tiegs, S.D., Cariss, H., Dobson, M., Elosegi, A., Ferreira, V., Graça, M.A., Fleituch, T., Lacoursière, J.O., Nistorescu, M., Pozo, J., Risnoveanu, G., Schindler, M., Vadineanu, A., Vought, L.B., Chauvet, E., 2012. Continental-scale effects of nutrient pollution on stream ecosystem functioning. Science 336 (6087), 1438–1440. https://doi.org/10.1126/science.1219534.